

Published in final edited form as:

Brain Res. 2004 August 13; 1017(0): 208–217. doi:10.1016/j.brainres.2004.05.049.

Excitatory and inhibitory local circuit input to the rat dorsal motor nucleus of the vagus originating from the nucleus tractus solitarius

Scott F. Davis^a, Andrei V. Derbenev^a, Kevin W. Williams^{a,b}, Nicholas R. Glatzer^a, and Bret N. Smith^{a,b,*}

^aDepartment of Cell and Molecular Biology, Division of Neurobiology, Tulane University, New Orleans, LA 70118, USA

^bNeuroscience Program, Tulane University, New Orleans, LA 70118, USA

Abstract

The nucleus tractus solitarius (NTS) and dorsal motor nucleus of the vagus nerve (DMV) constitute sensory and motor nuclei of the dorsal vagal complex, respectively. We used whole-cell patch-clamp recordings from DMV neurons in rat brain slices and three methods of stimulation (electrical, glutamate microdrop, glutamate photostimulation) to test the hypothesis that convergent excitatory and inhibitory inputs to DMV neurons originate from intact neurons in multiple NTS areas. Electrical stimulation of the NTS resulted in evoked excitatory and inhibitory postsynaptic currents (eEPSCs and eIPSCs) in DMV neurons. Stimulation of the dorsal NTS with glutamate microdrops, which selectively stimulates the soma and dendrites of intact neurons, resulted in 31% of DMV neurons receiving eEPSCs, 44% receiving eIPSCs, and 6% receiving convergent excitatory and inhibitory inputs. Glutamate photostimulation allowed selective activation of intact neurons in multiple, discrete areas of the NTS and resulted in 36% of DMV neurons receiving eEPSCs, 65% receiving eIPSCs and 20% receiving both inputs. Data obtained by stimulation of multiple NTS areas support the hypothesis that there are anatomically convergent inputs to DMV neurons originating from intact neurons within the NTS. These data support the hypothesis that there is transfer of convergent information from the NTS to the DMV, implying that significant sensory–motor processing occurs within the brainstem.

Keywords

GABA; Glutamate photostimulation; Patch-clamp; Reflex; Synaptic current

1. Introduction

The nucleus tractus solitarius (NTS) receives sensory information from cranial nerves VII, IX, and X. Sensory fibers of the vagus nerve innervating the gastrointestinal and cardiopulmonary systems are distributed in a loosely viscerotopic pattern onto neurons in the caudal NTS [1]. Viscerosensory afferents entering the NTS are joined by inputs from other CNS regions, resulting in an abundance of fibers of passage in the region [30,34]. A principal target of the processed NTS signal is assumed to be the adjacent dorsal motor nucleus of the vagus nerve (DMV). The DMV consists primarily of preganglionic

parasympathetic motor neurons innervating the subdiaphragmatic viscera. The apposition of sensory (i.e., NTS) and motor (i.e., DMV) components of the vagal complex has led to the hypothesis that synaptic connections between NTS and DMV neurons are a principal means of regulating visceral function.

Electrophysiological and anatomical experiments imply the existence of a connection between the NTS and DMV, which alters functional output of the vagus nerve onto, for example, gastrointestinal viscera [5,18,21,23,32,35]. Although most have focused on an inhibitory connection,[11,18,25,32] the existence of an excitatory connection has also been suggested [5,32]. Anatomical evidence for the existence of a direct connection between the NTS and DMV is based primarily on dye injections into the NTS [23], retrograde transneuronal viral labeling of NTS neurons after infection of terminal fields in the viscera [6,12], or morphological identification of neurons known to project to DMV [12]. However, these studies do not directly demonstrate synaptic connections between the nuclei and provide little information about the function or organization of connectivity with individual DMV cells.

Electrophysiological data supporting the direct NTS-to-DMV connection are mainly from experiments involving electrical stimulation of the NTS or activation of vagal afferents while recording from neurons of the DMV [11]. Electrical stimulation of the NTS depolarizes neurons, but also activates the numerous fibers of passage found through-out the dorsal vagal complex, including glutamatergic or GABAergic fibers originating from other brain areas. Data obtained from experiments using electrical stimulation of the brain parenchyma are therefore suggestive of synaptic connections between the NTS and DMV, but responses are just as likely to be due to activation of circuits bypassing or not originating in the NTS. Because selective activation of discrete local inputs to the DMV has not been addressed, it is not known whether individual cells in the DMV receive functionally convergent inputs (i.e., excitatory and inhibitory) arising from neurons within the NTS or if there are anatomically convergent inputs from multiple sites within the NTS onto individual DMV neurons. Such information is necessary in order to assess the relationships between sensory and motor systems controlling different components of the viscera. The cellular nature of the putative connections between the sensory and motor components of the vagal complex is uncertain and requires more detailed examination.

Chemical stimulation techniques have allowed investigators to reliably stimulate circuits whose cell bodies or dendrites are in the vicinity of the stimulus, while avoiding activation of fibers of passage. The glutamate microdrop technique involves pressure applying L-glutamate via a modified patch pipette directly onto cells [3,9,10,26]. This technique selectively depolarizes soma and dendrites, but not axons. Glutamate photostimulation involves focal release of glutamate using ultraviolet light projected into the slice [6,11,19,29,36]. This method of stimulation avoids physical contact with the slice and affords the advantage of being able to stimulate neurons at multiple, discrete sites within the slice. In the present study, these techniques were used to stimulate neurons in the NTS while performing whole-cell patch-clamp recordings of neurons in the DMV in order to more directly test the hypothesis that DMV neurons receive anatomically and functionally convergent inputs originating in the NTS.

2. Materials and methods

2.1. Slice preparation

Male Sprague-Dawley rats (Harlan, Indianapolis, IN) 4-8 weeks of age were housed under a standard 12-h light/dark cycle, with food and water provided ad libitum. All animals were treated and cared for in accordance with the rules of the Tulane University Animal Care and

Use Committee and NIH guidelines. Rats were deeply anesthetized with sodium pentobarbital (100 mg/kg, i.p.) or Halothane (Sigma, St. Louis, MO) inhalation and then decapitated while anesthetized. The brain was removed and blocked coronally, rostral to the cerebellum on an icecold stand. The brainstem was then glued to a sectioning stage with a cyanoacrylate-based adhesive. Similar to previous descriptions [11,13,28], transverse (i.e., coronal) brainstem slices (400 μm) containing the caudal vagal complex were made in 0–2 °C, oxygenated (95% O₂/5% CO₂) artificial cerebrospinal fluid (ACSF) using a vibrating microtome (Vibratome Series 1000; Technical Products Intl., St. Louis, MO). The ACSF contained (in mM): 124 NaCl, 3 KCl, 1.5 CaCl₂, 1.3 MgCl₂, 1.4 NaH₂PO₄, 26 NaHCO₃, 11 glucose; pH = 7.3–7.4, with an osmolality of 290–315 mosM/kg. Slices were equilibrated for at least 1 h in 33–35 °C oxygenated ACSF. A single slice was then transferred to a submersion style recording chamber on a fixed stage mounted under an upright (Olympus, BX50WI or BX51WI, Melville, NY) or an inverted (Nikon TE200, Melville, NY) microscope and continuously perfused with ACSF. The composition of the ACSF used for recordings was identical to that used in the dissection.

2.2. Electrophysiological recording

Whole-cell patch-clamp recordings were obtained in the DMV as described previously [11] using patch pipettes pulled from borosilicate glass capillaries of 0.45-mm wall thickness (Garner Glass, Claremont, CA), with open tip resistances of 3–5 M Ω . Pipettes were filled with (in mM): 130 K⁺-gluconate (or Cs⁺-gluconate), 1 NaCl, 5 EGTA, 10 HEPES, 1 MgCl₂, 1 CaCl₂, 3 KOH (or CsOH), 2–4 ATP; 0.2% biocytin; pH 7.2–7.4. Electrophysiological data were obtained using one of two recording configurations. Neurons were targeted for recording under a 40 \times water-immersion objective (numerical aperture = –0.8) using infrared-differential interference contrast (IR-DIC) optics (Olympus), visualized using a Spot RT Slider CCD camera (Diagnostic Instruments; Sterling Heights, MI) or a digital video camera. Other recordings were performed “blind” by guiding the recording pipette into the DMV using a dissecting microscope (Nikon) mounted above a recording chamber positioned over an inverted microscope (Nikon), which was used to direct light from a flash lamp into the slice.

Electrophysiological signals were recorded using either an Axopatch 200B, or Axopatch 1D, or Multiclamp 700A amplifier (Axon Instruments, Union City, CA). Signals were low pass filtered at 2–5 kHz, digitized at 88 kHz (Neurocorder, Cygnus Technology, Delaware Water Gap, PA), and recorded onto videotape and to a PC-style computer (Digidata 1320A, Axon Instruments). Data were captured using the pCLAMP program suite (Axon Instruments) and analyzed using pClamp or Mini-analysis (Synaptosoft, Decatur, GA). Once in the whole-cell configuration, cells were initially held near the resting membrane potential for 5–10 min to allow equilibration of the cytoplasm and recording electrode solution. Seal resistance was typically 2–4 G Ω and series resistance, measured from brief voltage steps (5 mV, 5 ms) applied through the recording pipette, was typically < 20 M Ω , and was monitored periodically during the recording. Recordings in which a >20% change in series resistance was measured during the recording period were excluded from the analysis. Input resistance was assessed by measuring the current at the end of brief voltage pulses of 5–10 mV or by determining the linear slope conductance from a voltage ramp protocol, as described previously [28]. Resting membrane potential was determined by periodically monitoring the voltage at which no current was measured (i.e., removing voltage-clamp control of the neuron by switching to $I = 0$) during the recording.

Electrical stimulation of the NTS (300 μs , 0.1 Hz) was performed using either a bipolar electrode made from a pair of teflon-coated platinum–iridium wires (75- μm diameter, f 100- μm tip separation) or a concentric bipolar platinum–iridium electrode (125- μm diameter; FHC, Bowdoinham, ME). Stimulation intensity was adjusted so that excitatory or inhibitory

postsynaptic currents (EPSCs or IPSCs) were evoked after >75% of the trials. Evoked EPSCs (eEPSCs) were examined at holding potentials between the resting membrane potential and the calculated Cl^- equilibrium potential (i.e., typically between -50 and -80 mV). Evoked IPSCs (eIPSCs) were examined at less negative holding potentials (-30 to 0 mV). In most experiments which examined eIPSCs, Cs^+ was present in the recording pipette, preventing voltage-dependent potassium currents and facilitating the voltage-clamp. The GABA_A antagonists, picrotoxin ($100 \mu\text{M}$) or bicuculline methiodide ($30 \mu\text{M}$) were applied to block IPSCs and to isolate excitatory responses from the possible effects of activating local GABAergic circuits. The glutamate AMPA/kainate receptor antagonist, 6-cyano-7-nitroquinoxaline-2,3-dione (CNQX; $10 \mu\text{M}$) and the NMDA receptor antagonist, DL-5-amino-phosphonovaleric acid (APV; $50 \mu\text{M}$; receptor antagonists all from Sigma) were applied to block EPSCs and to isolate inhibitory circuits from possible secondary activation of local glutamatergic circuits. Tetrodotoxin (TTX; $2 \mu\text{M}$) (Sigma; or Alomone Labs, Jerusalem, Israel) was added to the ACSF to block Na^+ -dependent action potentials.

2.3. Glutamate microdrops

L-glutamate was pressure applied (20 mM ; 10 ms ; 10 psi) through a patch pipette ($\sim 10\text{-}\mu\text{m}$ tip diameter) positioned just above the surface of the slice. The effectiveness of the glutamate in evoking action potentials was verified by applying the glutamate directly at the tip of the recording pipette to evoke unclamped, rapid voltage-dependent inward currents in the recorded neuron (i.e., the fast Na^+ currents underlying action potentials). In this configuration, recordings were made in the medial half of the DMV and glutamate was applied to the dorsal or dorsolateral NTS. Slices were positioned such that ACSF flowed toward the lateral or dorsal surface of the slice (i.e., away from DMV and NTS) to minimize direct effects when stimulating NTS. Direct application of glutamate to areas of the slice adjacent to the NTS did not result in synaptic responses in the DMV. Comparisons of eEPSC and eIPSC amplitude and frequency were compared for 5 s prior to and after each glutamate application. Frequency of evoked currents was defined as the difference between the number of currents in the 5 s prior to and immediately following glutamate application.

2.4. Glutamate photostimulation

Glutamate photostimulation was performed similar to previous descriptions [6,11]. L-glutamic acid, γ -(α -carboxy-2-nitrobenzyl) ester, trifluoroacetic acid salt (i.e., CNB-caged glutamate; $250 \mu\text{M}$ Molecular Probes, Eugene, OR), which does not bind to glutamate receptors, was added to recirculated, oxygenated ACSF. A xenon flash lamp (TILL Photonics, Eugene, OR) was used to uncage glutamate [6], which allowed the molecule to activate glutamate receptors at the site of uncaging. The flash of UV light ($2\text{--}3 \text{ ms}$) was directed through the epifluorescence port of an inverted microscope (Nikon TE200) and focused through the slice by positioning a high numerical aperture $40\times$ oil immersion objective (Nikon) beneath the cover glass that formed the floor of the recording chamber. A diode laser ($\lambda = 670 \text{ nm}$), which does not uncage the glutamate, was directed through the objective to aim the UV flash using the camera port on the microscope and viewed using a CCD camera attached to a dissecting microscope above the slice. The flash of UV light was directed into discrete areas to evoke glutamate-induced action potentials in NTS neurons.

Alternatively, photolysis was made using light from a mercury lamp directed through a UV filter set in the epifluorescence system of the fixed-stage upright microscope (Olympus BX50WI). An electronic shutter (Uniblitz, Vincent Associates, Rochester, NY) mounted in front of the light source allowed brief ($10\text{--}15 \text{ ms}$) UV illumination of the area of the slice under the $40\times$ water-immersion objective used to obtain recordings. For both uncaging systems, the effective diameter of glutamate photolysis ($< 100 \mu\text{m}$) was determined empirically by detecting direct inward currents caused by uncaging glutamate at the tip of

the recording pipette and then moving the flash area progressively farther away from the recording by manually moving the microscope. No response differences were apparent between the two photolysis configurations used. In control experiments, there was no degradation of the direct response (i.e., the inward current) after more than 100 stimuli.

Because glutamate uncaging activated local circuits and resulted in a barrage of action potential-evoked postsynaptic currents (PSCs), glutamate-evoked responses were analyzed by subtracting the baseline frequency of spontaneous PSCs before uncaging from the PSC frequency following uncaging. Therefore, the frequency of glutamate-evoked PSCs is defined as frequency of PSCs after uncaging minus frequency of spontaneous PSCs in the 10–30 s prior to uncaging. A paired Student's *t*-test was used to determine if the frequency of PSCs following glutamate photostimulation was significantly increased over baseline. Significance was set to $p < 0.05$. Numbers are expressed as means \pm standard error of the mean (S.E.M.). EPSCs and IPSCs evoked by glutamate photostimulation are action potential dependent and do not result merely from depolarization of nerve terminals since application of 2 μ M TTX abolished glutamate-evoked EPSCs and IPSCs [11].

3. Results

3.1. Electrical stimulation of the NTS-eEPSCs

Voltage-clamp recordings were performed in 48 DMV neurons while stimulating the NTS electrically to determine the types of synaptic inputs to DMV neurons. Electrical stimulation was used in 23 of these neurons to look for eEPSCs. Electrical stimulation of the NTS resulted in eEPSCs in 21 of these 23 neurons (91%) when voltage clamped at -61.6 ± 1.5 mV. Evoked EPSCs were usually unitary, but occasionally were accompanied by multiple evoked events (Fig. 1). The average amplitude of evoked EPSCs was -41.75 ± 9.27 pA. Evoked EPSCs had rapid rise times and exponential decays and were blocked by ionotropic glutamate receptor antagonists (CNQX 10 μ M; APV 50 μ M; $n = 11$), similar to previous studies [11,32].

3.2. Electrical stimulation of the NTS-eIPSCs

Another 42 neurons were voltage-clamped at more depolarized holding potentials to examine electrically evoked IPSCs. In 40 of the 42 neurons examined (95%), electrical stimulation of the NTS resulted in eIPSCs. Similar to what was seen for evoked EPSCs, electrical stimulation of the NTS usually resulted in a unitary IPSC, but occasionally secondary IPSCs were observed (Fig. 1). In some experiments ($n = 11$), 10 μ M CNQX was added to the ACSF to pharmacologically isolate IPSCs. The average amplitude of IPSCs evoked after electrical stimulation of the NTS at an average holding potential of -17.0 ± 1.5 mV was 36.5 ± 4.1 pA when CNQX was added and 69.8 ± 9.8 pA without CNQX. Evoked IPSCs also had rapid rise times and monoexponential decays and were blocked by picrotoxin (50–100 μ M) or bicuculline (10 μ M), similar to previous reports [11,32].

3.3. Electrical stimulation of the NTS—both eEPSCs and eIPSCs

The presence of both eEPSCs and eIPSCs was determined in 17 neurons and both types of input were observed in each of these cells (100%). Neurons were hyperpolarized (-50 to -80 mV) to examine EPSCs. The membrane potential was then depolarized (-30 to 0 mV) to detect IPSCs. Thus, nearly all individual DMV neurons received excitatory and/or inhibitory synaptic input after electrical activation of neurons and/or axons in the adjacent NTS region.

3.4. L-glutamate microdrops

Application of L-glutamate microdrops to the NTS also resulted in eEPSCs and eIPSCs in the DMV. L-glutamate microdrop stimulation was made in the dorsal NTS, far enough from the DMV to avoid directly stimulating the dendrites of the recorded neuron. Application in nearby areas of the slice outside of the NTS failed to elicit synaptic responses in any neuron ($n = 32$). Unlike synaptic responses observed after electrical stimulation, PSCs evoked using L-glutamate microdrops never occurred as single, unitary events. Instead the response consisted of a significant increase in the frequency of PSCs following L-glutamate application above the spontaneous PSC level observed prior to the application (Figs. 2 and 3).

A total of 32 neurons were examined for the presence of both eEPSCs and eIPSCs using L-glutamate microdrop stimulation of the NTS. At holding potentials near -70 mV, 10 neurons (31%) responded to application of L-glutamate with a barrage of eEPSCs (Fig. 2). The average eEPSC frequency measured in the first 5 s following stimulation was 15.8 ± 3.3 Hz ($n = 7$).

L-glutamate-evoked IPSCs were observed in 14 of 32 neurons (44%) examined at holding potentials near -20 mV (Fig. 3). The average frequency of eIPSCs measured in the first 5 s following stimulation was 28.2 ± 6.5 Hz (Fig. 3). In addition, 2 of 32 (6%) of neurons examined were observed to receive both eEPSCs and eIPSCs following L-glutamate application to the same place in the slice. Thus, 20% of cells receiving eEPSCs also received eIPSCs (i.e., 2 of 10 cells) and 14% of cells receiving eIPSCs also received eEPSCs (i.e., 2 of 14 cells). These data indicated that depolarization of NTS neurons by L-glutamate resulted in excitatory and inhibitory synaptic responses in the DMV.

3.5. Glutamate photostimulation

In order to test the hypothesis that synaptic inputs originating from different sites within the NTS converged onto single DMV neurons, we performed glutamate photo-stimulation in multiple areas of the NTS corresponding to previously identified functional NTS subnuclei [1]. Neurons were recorded in the DMV ($n = 33$) and glutamate was focally uncaged. Initially, neurons were voltage-clamped at resting membrane potential and glutamate was uncaged directly at the tip of the recording pipette, resulting in an inward current and/or a putative Na^+ -current (Fig. 4). The stimulation site was moved progressively away from the recorded neuron in approximately $50\text{-}\mu\text{m}$ increments until no inward current was detected. This was repeated in at least one other direction to establish the effective uncaging diameter in the slice, which was $50\text{--}100\ \mu\text{m}$ for all experiments. The glutamate photostimulation was then made at up to five distinctly separate positions within the NTS. These positions were classified according to their relative location within the nucleus as central, dorsomedial, dorsolateral, ventromedial, and ventrolateral (Figs. 4 and 5). Each DMV neuron was evaluated for the presence of either eEPSCs, eIPSCs, or both at one or more of these locations. Activation of local synaptic connections by glutamate photostimulation in the NTS resulted in eEPSCs in 5 of 14 (36%) of DMV neurons examined in normal ACSF (Fig. 4). In five additional neurons, GABAergic inhibition was blocked with $100\ \mu\text{M}$ of the GABA_A antagonist picrotoxin. In the presence of picrotoxin, eEPSCs were observed in four of the five neurons examined (80%). Another 26 neurons were examined for the presence of eIPSCs at depolarized holding potentials (-30 to 0 mV). Of these, 17 (65%) received eIPSCs originating from the NTS (Fig. 5). The presence of both eEPSCs and eIPSCs was determined in 10 neurons. Of these, two of the total (20%) were observed to receive both types of input, while six others received only eIPSCs and two received neither type of response. The presence of eIPSCs was tested for in three of the cells in which eEPSCs were

detected. Two of these three neurons also received eIPSCs. The two neurons that received both eEPSCs and eIPSCs received input from multiple NTS areas.

To determine if DMV neurons received anatomically convergent inputs originating from multiple locations within the NTS (Figs. 4 and 5; Table 1), we stimulated two or more areas of the NTS in each of the 5 neurons found to receive eEPSCs and 13 neurons that received eIPSCs. Of the five cells that received eEPSCs, three received eEPSCs originating from more than one area of the NTS. The remaining two neurons only received excitatory input after stimulation of the dorsomedial NTS. Inhibitory input converging from two to three different areas of the NTS was observed in 4 of 13 neurons, while the remaining nine received IPSCs from only one area. Moreover, there did not appear to be any region of the caudal NTS that was more likely to result in EPSCs or IPSCs when stimulated. However, neither excitatory nor inhibitory events were evoked from the ventrolateral NTS in any neuron examined (Table 1). Evoked responses were obtained from the central, dorsolateral, dorsomedial, and ventromedial regions of the caudal NTS (Table 1), and responses were observed in individual neurons after stimulation of multiple areas of the NTS.

4. Discussion

Vago-vagal reflexes appear to be mediated in large part by an inhibitory connection to the DMV, which is activated after viscerosensory afferent stimulation [18], but excitatory connections can also play a role. The NTS, however, does not serve simply as a relay nucleus, but as an autonomic regulatory center. Therefore, viscerosensory signals can be reconciled with descending and ascending inputs before influencing vagal motor output. Results from anatomical tracing studies and electrophysiological experiments utilizing electrical stimulation are consistent with the hypothesis that there is a local circuit connecting the NTS and DMV [5,21,23,32,35]. However, most of these experiments did not provide the resolution necessary to differentiate between connections originating from neurons within the NTS versus fibers of passage whose cell bodies may be outside the dorsal vagal complex, including vagal afferents [20,32]. Additionally, it is difficult or impossible to determine, using these techniques, if a single DMV neuron is capable of receiving functionally or anatomically convergent inputs originating in multiple sites within the NTS. We compared responses from electrical stimulation to those from glutamate microdrop application and glutamate photostimulation. Our results positively demonstrate the existence of an *intact* connection between the neurons in the NTS and the DMV. They also demonstrate that glutamatergic and GABAergic neurons in the NTS converge onto DMV cells. Finally, our results show that output from NTS neurons in disparate areas of the NTS converge onto single DMV neurons, providing a synaptic substrate to support the hypothesis that vagal reflexes in one organ system can be triggered by visceral afferents originating in the same or another system (see Ref. [22] for review).

Electrical stimulation of the NTS resulted in eEPSCs and eIPSCs in the DMV in almost every instance, supporting and expanding upon previous findings [4,5,12,17,23]. However, due to abundant axons in the caudal NTS and DMV arising from neurons in other CNS regions, from other levels of the NTS, or from the solitary tract, it is impossible to know if electrically evoked PSCs in the DMV were the result of activity arising from neurons of the caudal NTS. Many central neurons express GABA or glutamate in addition to neuromodulatory substances, including some diencephalic populations that project to the DMV. For example, hypocretin-immunoreactive terminals also colocalize glutamate [31], and these peptidergic axons, which originate from somata in the hypothalamus, are abundant in the DMV and NTS [28]. It has also been reported that the hypothalamic paraventricular nucleus sends a glutamatergic projection directly to the DMV, the fibers of which likely traverse the NTS [37]. Central amygdala inputs to the vagal complex that are somatostatin-

immunoreactive have also been reported to contain GABA [24]. In addition, putative direct gastric vagal afferents to the DMV pass through the NTS [20], offering another route for stimulation of fibers of passage rather than intact neuronal connections. Although responses in DMV neurons to electrical stimulation of the NTS are taken as evidence that an intact connection exists between the nuclei, it is very likely that synaptic input evoked by electrical stimulation originates from non-NTS as well as NTS sources.

Electrically evoked EPSCs and IPSCs were often unitary events. On occasion, especially with relatively low stimulus intensities, electrical stimulation resulted in an increased PSC frequency following the stimulus. One explanation for this is an increased frequency of action potentials occurring in intact neurons of the slice. The relatively smaller amplitude of evoked IPSCs in the presence of CNQX indirectly suggests the presence of an intrinsic excitatory connection onto intact neurons that enhances evoked IPSCs and was blocked by the glutamate receptor antagonist, but this connection remains uncharacterized. Conversely, unitary responses may be due to strong activation of fibers traversing the NTS near the stimulating electrode. Although they were not made in this study, previous estimates suggest the area activated by electrical stimulation in brain parenchyma can be on the order of up to 1 mm in diameter [15], which would be expected to activate large areas of the NTS. The input provided by fibers of passage may be sufficiently large to obscure more discrete inputs arising from NTS neurons.

Chemical stimulation techniques typically do not depolarize fibers of passage, allowing neuron cell bodies and dendrites to be selectively activated, as they contain ionotropic glutamate receptors [3,6,10,19,26]. We previously demonstrated an inhibitory connection between the NTS and DMV using glutamate photostimulation at a single point [11]. Synaptic responses after glutamate stimulation were blocked with TTX, indicating that action potentials were required for evoked synaptic responses, and the responses were not simply due to depolarization of axon terminals [11,19]. Application of L-glutamate microdrops delivers selective stimulation of neurons within the NTS, making the technique a valuable indicator of intact local synaptic connections. Unitary PSCs were never observed following stimulation of the NTS with glutamate microdrops. We hypothesize that unlike electrical stimulation, which can effectively stimulate fiber bundles and may mask the contribution of individual neurons, glutamate microdrops activated multiple action potentials in individual neurons or groups of neurons. Multiple action potentials in neurons are likely to have varying temporal properties which would preclude them from contributing to a constant latency unitary PSC.

When analyzing PSCs evoked by chemical stimulation, the background spontaneous frequency of events was subtracted from the increased frequency following the stimulation to determine the response, whereas amplitude and timing usually determine responses to electrical stimulation [4,11]. Because it is difficult to discern whether any specific event is evoked or spontaneous, we felt that analysis of amplitudes or latencies of glutamate-evoked polysynaptic inputs was probably not as reliable a measure as frequency change. Although we cannot be certain whether a response is mono- or polysynaptic, the hypothesis that action potentials generated within NTS neurons results in rapid synaptic responses in the DMV was supported.

Stimulation with glutamate microdrops does not necessarily facilitate examination of inputs arising from multiple sites within a slice because of the physical contact between the modified patch pipette containing the glutamate and the ACSF around the tissue. Based on our experience with direct glutamate applications to recorded neurons, the glutamate microdrops we used activated neurons in a region of approximately 200–400 μm in diameter, partially restricted by the direction of flow of the ACSF, which carried the

glutamate away from the slice. On the other hand, glutamate photostimulation allows for delivery of focal stimuli while allowing free movement of the stimulation site from place to place within the slice, since there is no physical contact with the tissue [6]. This technique allowed stimulation of multiple NTS sites of 50-100 μm diameter in order to test the hypothesis that individual neurons of the DMV receive anatomically convergent inputs originating in multiple regions of the NTS. The regions tested were classified as dorsomedial, dorsolateral, ventromedial, ventrolateral, and central, based on the location of previously described functional subnuclei [1,30]. It is likely that there is some degree of functional overlap between the defined areas, but the small area of glutamate uncaging likely produced a functionally discrete stimulation area. In addition, stimuli were separated by at least twice the effective uncaging diameter to ensure that different regions of the slice were activated by the glutamate.

Glutamate microdrop and photostimulation of the NTS revealed the presence of both excitatory and inhibitory inputs to the DMV. However, our data suggest that there is a predominance of inhibitory projections to the DMV originating from intact neurons of the NTS. This interpretation is based on the relatively larger probability of evoking IPSCs compared with EPSCs. There are possibly additional excitatory inputs to the DMV originating from NTS neurons that are tonically inhibited by GABAergic inputs [27]. Evidence for this is that an increase in eEPSC responses was seen in the presence of the GABA_A antagonist, picrotoxin. Picrotoxin likely causes a disinhibition of excitatory neurons in the NTS unmasking this projection. It is not clear when or if these inputs are active in vivo, but it is probable that disinhibition of a local excitatory circuit represents a tuning mechanism for modulating vagal output.

A minority of DMV neurons received both eEPSCs and eIPSCs indicating functionally convergent inputs originating from the NTS. It has been proposed that there are two major output pathways of the preganglionic parasympathetic motor neurons of the DMV [8,33]. One population of neurons projects via a cholinergic postganglionic parasympathetic pathway. Activation of this pathway results in an increase in motility of the proximal GI tract. The other population projects to the non-adrenergic, non-cholinergic (NANC) postganglionic neuron pathway, whose activation is generally thought to inhibit GI motility [5,16,38]. Based on this model, it has been hypothesized that DMV neurons projecting via the excitatory cholinergic pathway or the inhibitory NANC pathway receive primarily one type of input from the NTS (i.e., glutamate or GABA), depending on the final output of the pathway [33]. Considering that most neurons in which eEPSCs were observed also displayed eIPSCs and vice versa, it appears that most cells capable of receiving one type of synaptic input of NTS origin may also receive the other type. Considering the highly focal nature of the stimulation and the inherently limited architecture of a brain slice, it is likely that the percentage of neurons receiving both eEPSCs and eIPSCs from the NTS is an underestimation. We assume this accounts of the lack of responses originating from the ventrolateral NTS. It may be that convergent excitatory and inhibitory inputs allow one neuron to differentially modulate gastrointestinal or other visceral functions under different circumstances. The implication of functionally variable inputs may be to stimulate or inhibit gastrointestinal motility, depending upon a specific stimulus. The conditions under which each input dominates remain a question.

Many DMV neurons that responded to focal stimulation of the NTS received anatomically convergent inputs originating from multiple areas of the NTS. The implications of this may be important for understanding how putative vagovagal reflexes are organized within the DVC. Afferents from the stomach tend to localize to the dorsomedial NTS, whereas baroreceptor input is concentrated in the medial NTS, respiratory sensation in the ventrolateral NTS, and pharyngeal sensation in the intermediate NTS [1,14]. Dendrites from

any area might impinge on another area, so focal glutamate release—either from vagal afferent terminals or after glutamate photoactivation—might activate cells residing in another anatomical subdivision of the nucleus. Single DMV neurons often received input activated from more than one of these regions, implying that individual DMV cells might receive information regarding the sensory status of more than one component of a given visceral system, or even from more than one organ system. Using viral tracers, retrograde transynaptic labeling of NTS neurons following gastric infection indicated a widespread distribution of stomach-related NTS neurons in many subnuclei of the caudal NTS [7,13]. However, only the central NTS was labeled after esophageal inoculation [2]. Thus, it seems likely that synaptic connections within the DVC may integrate sensory-motor parasympathetic function across multiple visceral components. Identification of specific levels of inter-organ communication at the level of the DVC will help to clarify the functional implications of such an organization. At a minimum, it appears that NTS-to-DMV synaptic connections play an important role in coordinating parasympathetic motor output in addition to acting as a neurobiological substrate for vago-vagal reflexes.

Acknowledgments

This research was supported by NIH grants F32 MH064248 (SFD) and DK56132, NSF grant IBN-0080322 and American Heart Association grant 0030284N (BNS).

References

- [1]. Altschuler SM, Bao XM, Bieger D, Hopkins DA, Miselis RR. Viscerotopic representation of the upper alimentary tract in the rat: sensory ganglia and nuclei of the solitary and spinal trigeminal tracts. *J. Comp. Neurol.* 1989; 283:248–268. [PubMed: 2738198]
- [2]. Barrett RT, Bao X, Miselis RR, Altschuler SM. Brain stem localization of rodent esophageal premotor neurons revealed by transneuronal passage of pseudorabies virus. *Gastroenterology.* 1994; 107:728–737. [PubMed: 8076758]
- [3]. Boudaba C, Szabo K, Tasker JG. Physiological mapping of local inhibitory inputs to the hypothalamic paraventricular nucleus. *J. Neurosci.* 1996; 16:7151–7160. [PubMed: 8929424]
- [4]. Browning KN, Travagli RA. Characterization of the in vitro effects of 5-hydroxytryptamine (5-HT) on identified neurones of the rat dorsal motor nucleus of the vagus (DMV). *Br. J. Pharmacol.* 1999; 128:1307–1315. [PubMed: 10578146]
- [5]. Browning KN, Kalyuzhny AE, Travagli RA. Opioid peptides inhibit excitatory but not inhibitory synaptic transmission in the rat dorsal motor nucleus of the vagus. *J. Neurosci.* 2002; 22:2998–3004. [PubMed: 11943802]
- [6]. Callaway EM, Katz LC. Photostimulation using caged glutamate reveals functional circuitry in living brain slices. *Proc. Natl. Acad. Sci. U. S. A.* 1993; 90:7661–7665. [PubMed: 7689225]
- [7]. Card JP, Rinaman L, Schwaber JS, Miselis RR, Whealy ME, Robbins AK, Enquist LW. Neurotropic properties of pseudorabies virus: uptake and transneuronal passage in the rat central nervous system. *J. Neurosci.* 1990; 10:1974–1994. [PubMed: 2162388]
- [8]. Chang HY, Mashimo H, Goyal RK. Musings on the Wanderer: What's new in our understanding of vago-vagal reflex? IV. Current concepts of vagal efferent projections to the gut. *Am. J. Physiol., Gastrointest. Liver Physiol.* 2003; 284:G357–G366. [PubMed: 12576302]
- [9]. Christian EP, Dudek FE. Characteristics of local excitatory circuits studied with glutamate microapplication in the CA3 area of rat hippocampal slices. *J. Neurophysiol.* 1988; 59:90–109. [PubMed: 2893832]
- [10]. Christian EP, Dudek FE. Electrophysiological evidence from glutamate microapplications for local excitatory circuits in the CA1 area of rat hippocampal slices. *J. Neurophysiol.* 1988; 59:110–123. [PubMed: 2893830]
- [11]. Davis SF, Williams KW, Xu W, Glatzer NR, Smith BN. Selective enhancement of synaptic inhibition by hypocretin (orexin) in rat vagal motor neurons: implications for autonomic regulation. *J. Neurosci.* 2003; 23:3844–3854. [PubMed: 12736355]

- [12]. Ferreira M Jr, Browning KN, Sahibzada N, Verbalis JG, Gillism RA, Travagli RA. Glucose effects on gastric motility and tone evoked from the rat dorsal vagal complex. *J. Physiol.* 2001; 536:141–152. [PubMed: 11579164]
- [13]. Glatzer NR, Hasney CP, Bhaskaran MD, Smith BN. Synaptic and morphologic properties in vitro of premotor rat nucleus tractus solitarius neurons labeled transneuronally from the stomach. *J. Comp. Neurol.* 2003; 464:525–539. [PubMed: 12900922]
- [14]. Kalia M, Sullivan JM. Brainstem projections of sensory and motor components of the vagus nerve in the rat. *J. Comp. Neurol.* 1982; 211:248–265. [PubMed: 7174893]
- [15]. Klemfuss H, Young SJ, Groves PM. Do antidromic latency jumps indicate axonal branching in nigrostriatal and hypothalamo-neurohypophysial neurons? *Brain Res.* 1987; 409:197–203. [PubMed: 3580868]
- [16]. Krowicki ZK, Sharkey KA, Serron SC, Nathan NA, Hornby PJ. Distribution of nitric oxide synthase in rat dorsal vagal complex and effects of microinjection of nitric oxide compounds upon gastric motor function. *J. Comp. Neurol.* 1997; 377:49–69. [PubMed: 8986872]
- [17]. Lewis MW, Hermann GE, Rogers RC, Travagli RA. In vitro and in vivo analysis of the effects of corticotropin releasing factor on rat dorsal vagal complex. *J. Physiol.* 2002; 543:135–146. [PubMed: 12181286]
- [18]. McCann MJ, Rogers RC. Impact of antral mechanoreceptor activation on the vago-vagal reflex in the rat: functional zonation of responses. *J. Physiol.* 1992; 453:401–411. [PubMed: 1464835]
- [19]. Pettit DL, Helms MC, Lee P, Augustine GJ, Hall WC. Local excitatory circuits in the intermediate gray layer of the superior colliculus. *J. Neurophysiol.* 1999; 81:1424–1427. [PubMed: 10085368]
- [20]. Rinaman L, Card JP, Schwaber JS, Miselis RR. Ultrastructural demonstration of a gastric monosynaptic vagal circuit in the nucleus of the solitary tract in rat. *J. Neurosci.* 1989; 9:1985–1996. [PubMed: 2723763]
- [21]. Rogers RC, McCann MJ. Intramedullary connections of the gastric region in the solitary nucleus: a biocytin histochemical tracing study in the rat. *J. Auton. Nerv. Syst.* 1993; 42:119–130. [PubMed: 8450172]
- [22]. Rogers RC, McTigue DM, Hermann GE. Vagal control of digestion: modulation by central neural and peripheral endocrine factors. *Neurosci. Biobehav. Rev.* 1996; 20:57–66. [PubMed: 8622830]
- [23]. Rogers RC, Hermann GE, Travagli RA. Brainstem pathways responsible for oesophageal control of gastric motility and tone in the rat. *J. Physiol.* 1999; 514:369–383. [PubMed: 9852320]
- [24]. Saha S, Henderson Z, Batten TF. Somatostatin immunoreactivity in axon terminals in rat nucleus tractus solitarius arising from central nucleus of amygdala: coexistence with GABA and postsynaptic expression of sst2A receptor. *J. Chem. Neuroanat.* 2002; 24:1, 13. [PubMed: 12084407]
- [25]. Sivarao DV, Krowicki ZK, Hornby PJ. Role of GABAA receptors in rat hindbrain nuclei controlling gastric motor function. *Neurogastroenterol. Motil.* 1998; 10:305–313. [PubMed: 9697105]
- [26]. Smith BN, Dudek FE. Network interactions mediated by new excitatory connections between CA1 pyramidal cells in rats with kainate-induced epilepsy. *J. Neurophysiol.* 2002; 87:1655–1658. [PubMed: 11877537]
- [27]. Smith BN, Dou P, Barber WD, Dudek FE. Vagally evoked synaptic currents in the immature rat nucleus tractus solitarius in an intact in vitro preparation. *J. Physiol. (Lond.)* 1998; 512:149–162. [PubMed: 9729625]
- [28]. Smith BN, Davis SF, Van Den Pol AN, Xu W. Selective enhancement of excitatory synaptic activity in the rat nucleus tractus solitarius by hypocretin 2. *Neuroscience.* 2002; 115:707–714. [PubMed: 12435409]
- [29]. Strecker GJ, Wuarin JP, Dudek FE. GABAA-mediated local synaptic pathways connect neurons in the rat suprachiasmatic nucleus. *J. Neurophysiol.* 1997; 78:2217–2220. [PubMed: 9325388]
- [30]. Swanson LW, Kuypers HG. The paraventricular nucleus of the hypothalamus: cytoarchitectonic subdivisions and organization of projections to the pituitary, dorsal vagal complex, and spinal

- cordas demonstrated by retrograde fluorescence double-labeling methods. *J. Comp. Neurol.* 1980; 194:555–570. [PubMed: 7451682]
- [31]. Torrealba F, Yanagisawa M, Saper CB. Colocalization of orexin a and glutamate immunoreactivity in axon terminals in the tuberomammillary nucleus in rats. *Neuroscience.* 2003; 119:1033–1044. [PubMed: 12831862]
- [32]. Travagli RA, Gillis RA, Rossiter CD, Vicini S. Glutamate and GABA-mediated synaptic currents in neurons of the rat dorsal motor nucleus of the vagus. *Am. J. Physiol.* 1991; 260:G531–G536. [PubMed: 1672243]
- [33]. Travagli RA, Hermann GE, Browning KN, Rogers RC. Musings on the wanderer: what's new in our understanding of vago-vagal reflexes? III. Activity-dependent plasticity in vago-vagal reflexes controlling the stomach. *Am. J. Physiol., Gastrointest. Liver Physiol.* 2003; 284:G180–G187. [PubMed: 12529266]
- [34]. van der Kooy D, Koda LY, McGinty JF, Gerfen CR, Bloom FE. The organization of projections from the cortex, amygdala, and hypothalamus to the nucleus of the solitary tract in rat. *J. Comp. Neurol.* 1984; 224:1–24. [PubMed: 6715573]
- [35]. Willis A, Mihalevich M, Neff RA, Mendelowitz D. Three types of postsynaptic glutamatergic receptors are activated in DMNX neurons upon stimulation of NTS. *Am. J. Physiol.* 1996; 271:R1614–R1619. [PubMed: 8997360]
- [36]. Wuarin JP, Dudek FE. Excitatory synaptic input to granule cells increases with time after kainate treatment. *J. Neurophysiol.* 2001; 85:1067–1077. [PubMed: 11247977]
- [37]. Zhang X, Fogel R. Glutamate mediates an excitatory influence of the paraventricular hypothalamic nucleus on the dorsal motor nucleus of the vagus. *J. Neurophysiol.* 2002; 88:49, 63. [PubMed: 12091532]
- [38]. Zheng ZL, Rogers RC, Travagli RA. Selective gastric projections of nitric oxide synthase-containing vagal brainstem neurons. *Neuroscience.* 1999; 90:685–694. [PubMed: 10215170]

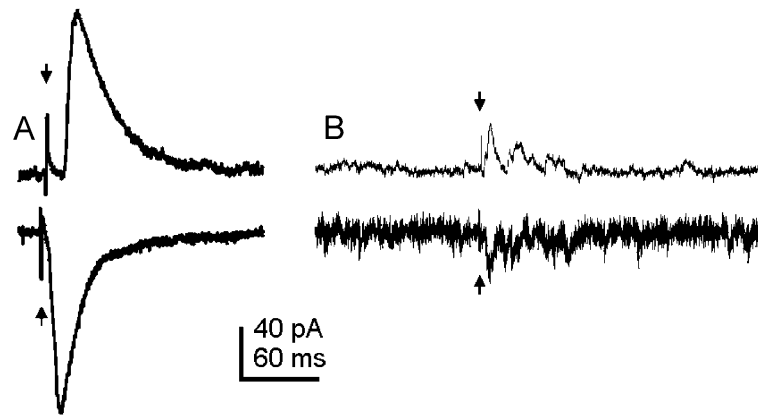


Fig. 1. Electrical stimulation of the NTS evoked EPSCs and IPSCs in DMV neurons. (A) Electrical stimulation of the NTS (arrows) resulted in a single constant-latency eIPSC (top trace) or eEPSC (bottom trace). An average of 14 traces from a whole-cell recording of a DMV neuron voltage-clamped at -20 mV (top) and 12 traces from a whole-cell recording of a different DMV neuron voltage-clamped at -75 mV (bottom) are shown. (B) Electrical stimulation of the NTS (arrows) resulted in a transient increase in frequency of IPSCs (top trace) or EPSCs (bottom trace). Both traces were obtained from the same neuron voltage-clamped at -20 mV (top) and -60 mV (bottom).

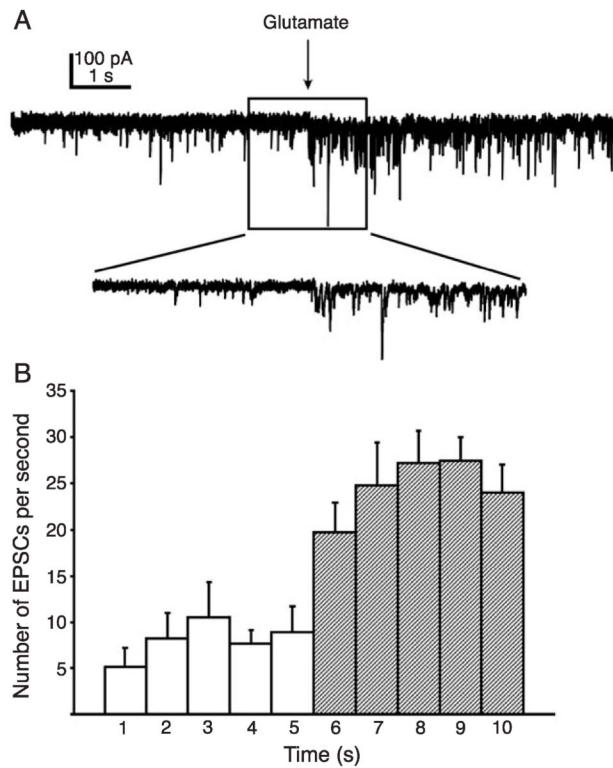


Fig. 2. Glutamate microdrop stimulation of the NTS resulted in evoked EPSCs in the DMV. (A) Application of L -glutamate (20 mM, 10ms) to the surface of the NTS produced a barrage of EPSCs recorded from a DMV neuron voltage-clamped at -70 mV. Inset: an expansion of part of the trace near the glutamate application (arrows). (B) Average number of eEPSCs during 1-s time intervals before and after application of glutamate (arrow; $n = 7$). Error bars indicate S.E.M. Each bin after the arrow represents a significant increase in EPSC frequency ($p < 0.05$).

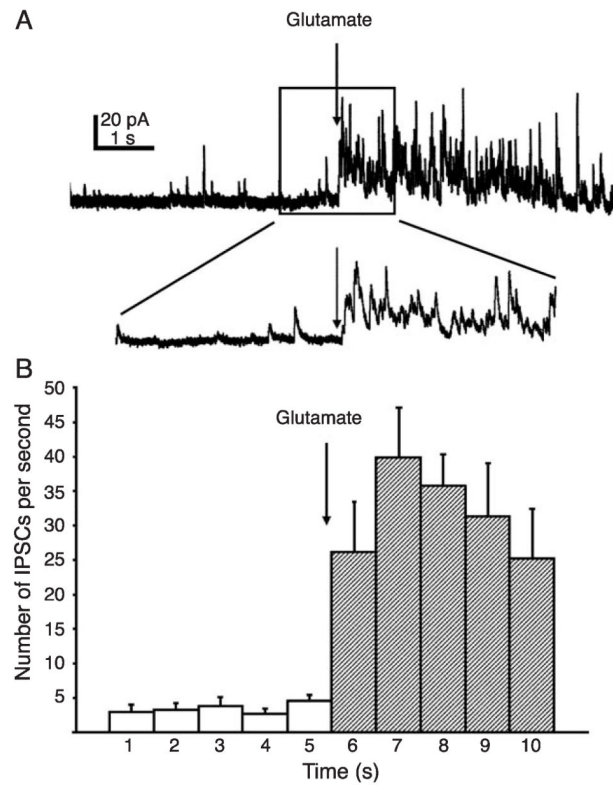


Fig. 3. Glutamate microdrop stimulation of the NTS resulted in evoked IPSCs in the DMV. (A) Application of glutamate (20 mM, 10 ms arrow) to the surface of the NTS produced a barrage of IPSCs recorded from a DMV neuron voltage-clamped at -20 mV. Inset: an expansion of part of the trace near the glutamate application (arrow). (B) Average number of IPSCs during 1-s binned time intervals before and after application of glutamate ($n = 7$ cells). Error bars indicate S.E.M. Post-glutamate frequency increase was significant ($p < 0.05$).

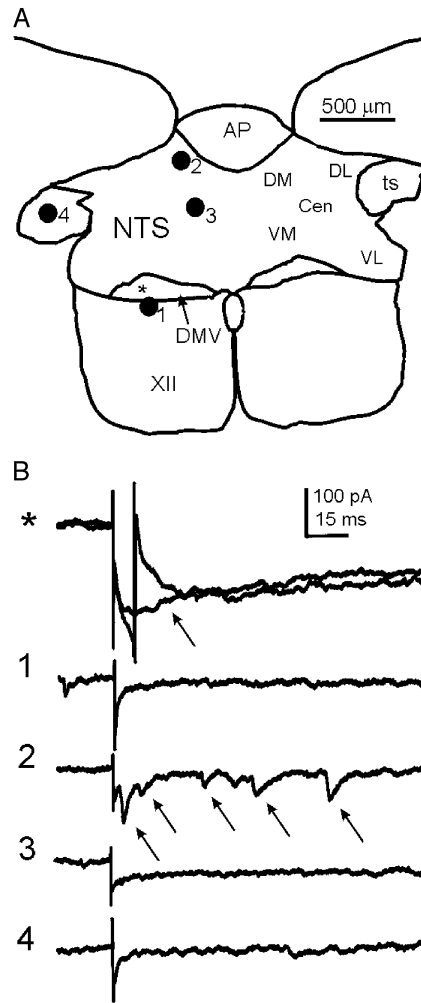


Fig. 4. Uncaging glutamate in discrete loci of the NTS evoked EPSCs in the DMV. (A) Diagram showing a representative transverse slice through the brainstem containing the dorsal vagal complex from which a DMV neuron was recorded. Numbered filled circles correspond to discrete loci where glutamate was uncaged in the slice. The position of the recorded neuron is indicated with an asterisk. The stimulation areas used in these experiments are indicated to the right. (B) Traces obtained from a whole-cell recording of a neuron voltage-clamped at -70 mV in the DMV whose position corresponds to the asterisk in A. The numbers to the left correspond to the loci in the NTS where glutamate was uncaged. The time of uncaging is indicated by the stimulus artifact in each trace. When glutamate was uncaged directly on the recorded neuron (asterisk) a sodium spike (arrow in first set of traces) was recorded in most trials. Shown are two consecutive stimulations, one of which evoked a sodium current. The cell also responded to glutamate uncaging in position 2 with an increase in EPSC frequency (arrows), but not in other positions. In this cell, glutamate was uncaged in all five areas, but only elicited an excitatory synaptic response when stimuli were applied to the dorsomedial NTS. Abbreviations: DM dorsomedial, DL dorsolateral, VL ventrolateral, VM ventromedial, CEN central, AP area postrema, ts tractus solitarius, XII hypoglossal nucleus, cc central canal.

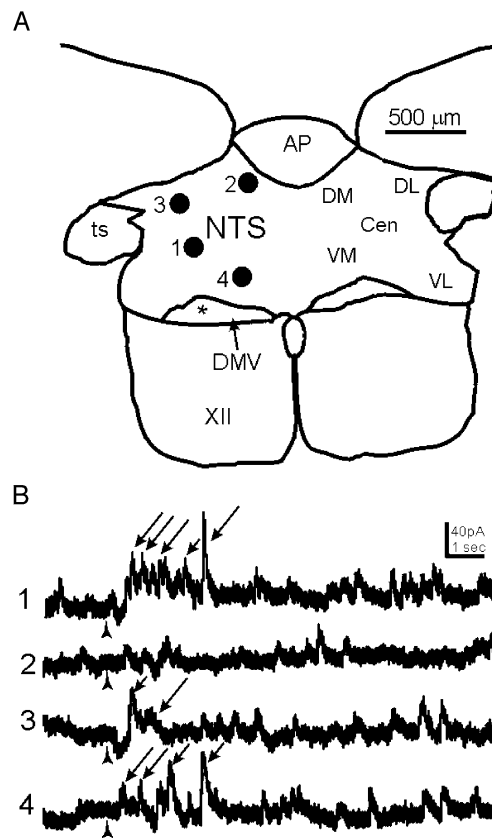


Fig. 5. Uncaging glutamate in discrete loci of the NTS evoked IPSCs in the DMV. (A) Diagram showing a representative transverse slice through the brainstem containing the dorsal vagal complex from which a DMV neuron was recorded. Numbered filled circles correspond to discrete loci where glutamate was uncaged in the slice. (B) Traces obtained from a whole-cell recording of a DMV neuron voltage-clamped at 0 mV. The numbers to the left correspond to the loci in the NTS where glutamate was uncaged. The time of uncaging is indicated by the arrowhead. Positions 1, 3 and 4 show examples of increased IPSC frequency following photostimulation in the NTS (arrows).

Table 1

Percentage of DMV neurons from which EPSCs and IPSCs were evoked by glutamate photostimulation from five different areas of the NTS

Area of NTS stimulated	eEPSC	eIPSC
Dosomedial	50%, <i>n</i> = 8	47%, <i>n</i> =15
Dorsolateral	20%, <i>n</i> = 5	42%, <i>n</i> =12
Ventromedial	25%, <i>n</i> = 8	31%, <i>n</i> =13
Ventrolateral	0%, <i>n</i> = 6	0%, <i>n</i> =9
Central	25%, <i>n</i> = 4	20%, <i>n</i> =10